Biochimica et Biophysica Acta, 548 (1979) 520—535

BBA 47771

TRANSFER OF LIGHT-INDUCED ELECTRON-SPIN POLARIZATION FROM THE INTERMEDIARY ACCEPTOR TO THE PREREDUCED PRIMARY ACCEPTOR IN THE REACTION CENTER OF PHOTOSYNTHETIC BACTERIA

P. GAST and A.J. HOFF

Department of Biophysics, Huygens Laboratory of the State University, P.O. Box 9504, 2300 RA Leiden (The Netherlands)

(Received April 12th, 1979)

Key words: Bacterial photosynthesis; ESR; Reaction center; Spin polarization; Electron acceptor

Summary

In reaction centers and chromatophores of photosynthetic bacteria strong light-induced emissive ESR signals have been found, not only after a flash, but also under continuous illumination. The signal, with $g = 2.0048$ and $\Delta H_{pp} = 7.6$ G, is only present under reducing conditions in material in which the primary acceptor, ubiquinone, U and its associated high-spin ferrous ion are magnetically uncoupled. Its amplitude under continuous illumination is strongly dependent on light intensity and on microwave power.

The emissive signal is attributed to the prereduced primary acceptor, U^-, which becomes polarized through transfer of spin polarization by a magnetic exchange interaction with the photoreduced, spin polarized intermediary acceptor, I^-. A kinetic model is presented which explains the observed dependence of emissivity on light intensity and microwave power. Applying this analysis to the light saturation data, a value of the exchange rate between I^- and U^- of $4 \cdot 10^8$ s^{-1} is derived, corresponding to an exchange interaction of 3—5 G.

Introduction

In recent years a number of studies have been devoted to the phenomenon of light-induced electron-spin polarization of doublet ESR signals in photosynthetic material [1—4]. These studies have a two-fold importance. First, from the shape of the polarized ESR lines one can, in principle, derive the

Abbreviations: ESR, electron spin resonance; SDS, sodium dodecyl sulphate; Mops, 3-(*N*-morpholino)-propanesulfonic acid.

multiplicity of the excited state of the primary donor from which an electron is photo-ejected in the act of light-induced charge separation. Secondly, electron-spin polarization depends on a subtle interplay of lifetimes of radical species and their magnetic interaction, so that the study of this phenomenon in photosynthetic material yields information on the structural geometry of the donor-acceptor complex.

Originally, it was concluded from the polarized signals of chloroplasts [1] and algae [2], that in these materials charge separation took place from a triplet excited state. Subsequently, polarized ESR signals were discovered in bacterial reaction centers, and it was demonstrated that they could only be explained assuming a singlet excited state as the precursor of charge separation [3]. Polarization then may develop by the socalled radical pair mechanism. The radical pair mechanism is well-known from the chemical literature on electron-spin polarization effects of radicals in solution (see for an introduction e.g. Refs. 5—7); under suitable conditions it can be operative in the solid state as well [3,8,9]. More recent work on plant material now suggests that in these systems also, the radical pair mechanism is responsible for the observed polarized ESR signals [4,10—12].

Another manifestation of the radical pair mechanism is the photoproduction of a polarized triplet ESR signal in reaction centers, chromatophores and intact cells of photosynthetic bacteria in which the primary acceptor is chemically reduced before illumination [13]. The polarization pattern [14], the dependence of the triplet yield on an applied magnetic field [6,7] and fast optical spectroscopic studies [15,16] all strongly suggest that the triplet arises from the back reaction $P^+I^- \rightarrow P^TI$, and that its yield depends on the dephasing of the electron-spins of P^+ and I^-.

From the study of electron-spin polarization in the bacterial photosystem, it transpires that in reaction centers polarization only develops, if in the primary acceptor (which in intact systems consists of a complex of a quinone and a high-spin ferrous ion) the magnetic interaction between the quinone and the iron is destroyed. The quinone which in this state acts as the primary acceptor is labelled U. Because of the strong influence of this magnetic coupling on the electron-spin polarization observed for doublet ESR signals, it seemed worthwhile to investigate the effect of the absence of the interaction on the induction of this triplet state P^T. In the course of these studies we have found quite unexpectedly a strongly emissive ESR line at $g = 2.0048$ with width $\Delta H = 7.6$ G, both after a light flash and under continuous illumination. In this report we present evidence that the emissive line arises from the emissively polarized primary acceptor, U^-, whose polarization develops as a result of exchange interaction between the reduced intermediary acceptor, I^-, and U^-. We present a simple model of the transfer of electron-spin polarization between I^- and U^- and show that it explains the observed dependence of emissivity on the intensity of the actinic light and on microwave power. A value of the exchange rate of about $4 \cdot 10^8\ s^{-1}$ is derived, which agrees well with the value estimated from the magnetic interaction between I^- and U^- in systems in which I^- can be accumulated [17].

A preliminary account of this work was presented on the 4th International Congress on Photosynthesis, Reading, England [18].

Materials and Methods

a. General

Bacteria were grown as described [19—21]. Chromatophores of *Rps. sphaeroides*, *R. rubrum* and *Rps. viridis* were obtained by sonication and differential centrifugation [22]. Reaction centers of wild type *Rps. sphaeroides*, labelled AUT-s particles, were prepared according to the method of Loach et al. [23] as modified by Slooten [24,25]. In this procedure, reaction center protein is solubilized by 0.3% SDS, and then centrifuged according to Loach [23] in the presence of 1 M urea and 0.3% Triton X-100 at pH = 10. The reaction centers are fully active at room temperature as compared with chromatophores; at 100 K their activity is 45% of that at room temperature. Reaction centers of the mutant *Rps. sphaeroides* R-26, kindly provided by Dr. G. Feher, were prepared according to the procedure of Okamura et al. [26]. The spectral properties of the reaction center preparations conform to the literature. For reaction centers of R-26, $\epsilon_{280}/\epsilon_{800} = 1.22 \pm 0.02$, showing that they contained little protein besides the reaction center protein [26]. 'Iron-depleted' reaction centers of R-26 were made according to the method of Feher et al. [27]; for some experiments a simplified procedure was adopted, in which reaction centers or chromatophores were incubated for about one hour at room temperature in the presence of 0.3% SDS. Ascorbate was added as a solid to a concentration in the range of 0.3—100 mM. In this range there was no effect of the ascorbate concentration on the experimental results. Dithionite was added in excess under anaerobic conditions using 10 mM morpholinopropane sulfonic acid (Mops) as a buffer. 2,3,5,6-Tetramethyl-*p*-phenylene diamine was dissolved in an ethanol-water mixture (50 : 50, v/v) and added to concentrations up to 100 μM. Stock solutions of ubiquinone (coenzyme Q_{10}) in 10% lauryl dimethylamine oxide (a gift from Onyx Corp.) were prepared by 10 min. sonication. Aliquots were added to the reaction center preparations to give a ubiquinone concentration of 250 μM and a lauryl dimethylamine oxide concentration of the final solution of less than 0.3%.

Absorption difference spectra at room temperature were measured using an absorption difference spectrometer previously described [28]. ESR experiments at temperatures down to 5 K were carried out with a Varian E-9 spectrometer typically working at 9.1 GHz, equipped with an Oxford Instrument helium gas-flow cryostat. The microwave power incident on the cavity was calibrated using a HP 8482A power meter, taking care to avoid impedance mismatch between the microwave power meter and the waveguide. Attenuation of 0 dB corresponded to 200 ± 5 mW microwave power in the frequency range of 9.0 to 9.5 GHz. The response time of the ESR spectrometer was shortened to 20 μs, measured as the risetime of the flash-induced triplet state (P^T) [13,29,30] in reduced chromatophores of *Rps. sphaeroides*, by removal of a low-pass filter in the 100 kHz lock-in detector [3,31]. The kinetic traces were obtained by accumulating at least 20 times randomly with respect to the phase of the field modulation. This gives the proper slope of the ESR line even at response times close to the inverse of the modulation frequency. The detection crystal was biased with a reference arm tuned to the out-of-phase component χ'' of the susceptibility, thus ensuring observation of the absorptive part of the

susceptibility. g-Values were measured using an AEG NMR Gauss meter and a frequency counter type HP 5246L equipped with a 12.4 GHz plug-in type HP 5255 A. Averageing, registration and further mathematical manipulations of the ESR signal were carried out employing a LSI/11 microprocessor interfaced with a PDP 11/10 and PDP 11/45 computer.

For light saturation ESR experiments a 1000 W Aldis projection lamp was used as the light source, filtered by 5 cm water and a HA-3 heat absorbing filter. Light intensities incident on the slotted cavity were calibrated using a YSI radiometer. For flash excitation either a Xenon flash tube or a Zeiss dye laser operating at 600 nm was used. For the ESR experiments the AUT-s particles were concentrated to an absorbance of 5 per cm at 800 nm by centrifugation for 20 h at 200 000 $\times g$. For light saturation experiments 50% glycol was added and the concentration was lowered to an absorbance of 1 per cm at 800 nm. The sample was contained in a quartz tube of 3 mm internal diameter. Before freezing to 5 K the samples were frozen to −190°C in the nitrogen flow cryostat. This procedure gives a homogeneous freezing and avoids the danger of breaking the ESR sample tube while warming up. The average number of light quanta absorbed by a sample inside the cavity was measured by monitoring the light saturation of P^+ in a sample containing AUT-s particles at 5 K. Assuming that the signal intensity is governed by the equilibrium

$$P \underset{k_{-1}}{\overset{k_L}{\rightleftharpoons}} P^+$$

with $k_{-1} = 33\ s^{-1}$ [32], a plot of $1/I_L$ versus $1/S$ (S is the ESR signal intensity, I_L is the incident light intensity in mW/cm^2) yields the number of quanta absorbed per second, k_L. Pre-illumination of samples containing ascorbate or DAD before and/or during freezing was carried out using a 500 W Aldis projection lamp as the light source and a nitrogen gas-flow cryostat. With this method the samples froze to −190°C within 6 s.

Samples containing ascorbate that were stored under liquid nitrogen did not show any loss of activity after 18 months of conservation; samples containing dithionite as a reductant could be conserved only for 3 months at 77 K without significant loss of activity.

b. Detection of spin polarization with ESR

The decay of spin polarized ESR signals depends on the spin lattice relaxation time T_1, on the chemical decay rate of the paramagnetic species and on the relaxation induced by emission or absorption stimulated by the microwave field. In the solid state, and at low temperatures the latter decay mechanism becomes dominant, and the decay time of the polarized ESR signal becomes strongly dependent on the microwave power [31]. Under these circumstances the effective decay time of the polarization is given by [33]:

$$T_{eff}^{-1} = T_1^{-1} + \frac{(\gamma H_1)^2 T_2}{1 + (\delta\omega T_2)^2} \tag{1}$$

in which T_2 is the transverse or spin-spin relaxation time, $\delta\omega$ is the offset from the resonance frequency, γ the magnetogyric ratio and H_1 the amplitude of the microwave magnetic field inside the sample. In the derivation of Eqn. 1 it is

assumed that $T_1 >> T_2$. It follows that for light-induced polarized signals the intensity and the line shape may strongly depend on the microwave power. These effects are carefully explored in the present work and our conclusions are based on results extrapolated to zero microwave power. At low temperatures, when T_1^{-1} becomes smaller than the modulation frequency, passage effects may occur [34]. The conditions for which these undesired effects become apparent depend on a combination of modulation frequency, spin-spin and spin-lattice relaxation times, and the rate at which the magnetic field is varied. Although the combination of high modulation frequency and a slow T_1, is not sufficient per se to yield passage effects [35], we have carefully checked for their occurrence by varying the experimental parameters, as temperature, modulation frequency, scanning rate, etc. We conclude that under our experimental conditions they are unimportant.

Results

Ambient redox potentials

AUT-s particles of *Rps. sphaeroides* which were used for the main body of experiments have been characterized by ESR and optical techniques [3,22,24,25]. When no special care was taken for absolute dark adaptation, we found in the dark in AUT-s particles at ambient redox potentials a weak ESR signal with a g-value of $g = 2.0028 \pm 0.0002$ (Fig. 1). This signal presumably is

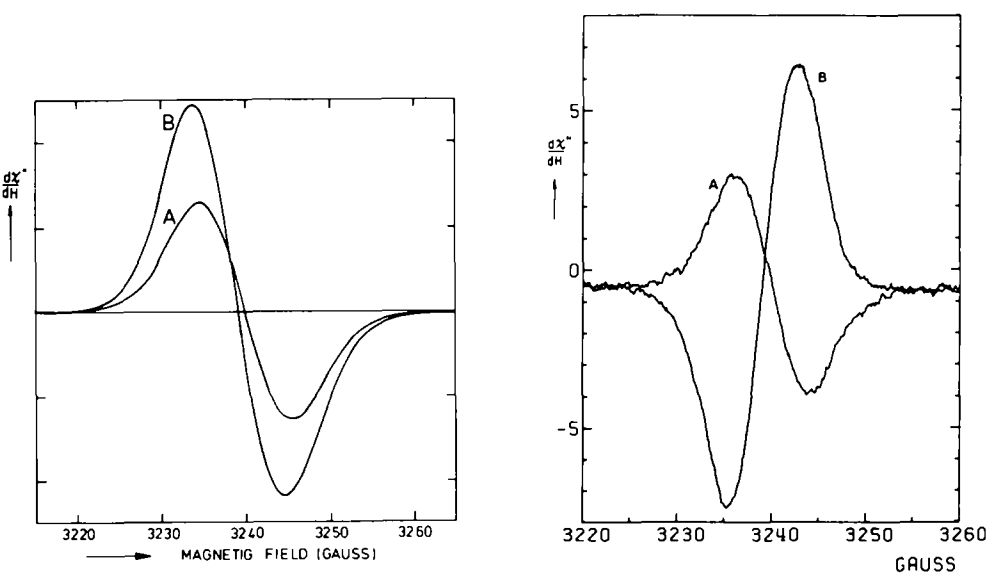

Fig. 1. Dark (A) and light (B) ESR signal measured at 5 K of AUT-s particles at ambient redox potential. Instrumental conditions: microwave frequency 9.1 GHz, microwave power 10^{-3} W, modulation amplitude 5 G, illumination with continuous white light.

Fig. 2. A. Dark ESR signal at 5 K of AUT-s particles which after addition of ascorbate were frozen in the light. B. The emissive signal that arises when the sample of AUT-s particles, prepared as in Fig. 2A, is illuminated at 5 K. Microwave power $2 \cdot 10^{-5}$ W.

due to a residual amount of oxidized primary donor, P^+. When such a sample was illuminated at 5 K a signal emerged with $g = 2.0035 \pm 0.0002$. This signal is attributed to the sum of the signal of P^+ ($g = 2.0026$) and that of the reduced primary acceptor ($g = 2.0048$) consisting of a ubiquinone from which the high-spin iron is uncoupled [27,36]. At 5 K both these signals started to saturate at a microwave power level of 2 mW. The structure of the acceptor complex was further investigated by optical spectroscopy following Vermeglio [37] and Wraight [38]. The absorbance change at 450 nm of R-26 reaction centers in the presence of 2,3,5,6-tetramethyl-*p*-phenylene diamine and ubiquinone after flash excitation showed oscillations with a periodicity of two as a function of flash number but the AUT-s particles showed no oscillations. This indicates that in the AUT-s particles either the secondary ubiquinone, U_2, is dissociated from the reaction center, or that electron transport from the primary acceptor, U_1, to U_2 is inhibited, possibly because of the absence of a functional high-spin iron [39].

Reducing conditions

AUT-s particles in the presence of ascorbate were frozen to 77 K under continuous illumination. The dark ESR signal at 5 K consisted of a slightly asymmetric line at $g = 2.0048 \pm 0.0002$ with a peak-to-peak linewidth of 7.9 ± 0.4 G (measured a 80 dB attenuation, Fig. 2). These values indicate that the dark signal is due to reduced U_1 from which the high-spin iron is uncoupled. This was confirmed by a low temperature Q-band (35 GHz) ESR spectrum of this signal, which showed the characteristic lineshape of the frozen semiquinone radical [27]. The dark signal started to saturate at remarkably low microwave

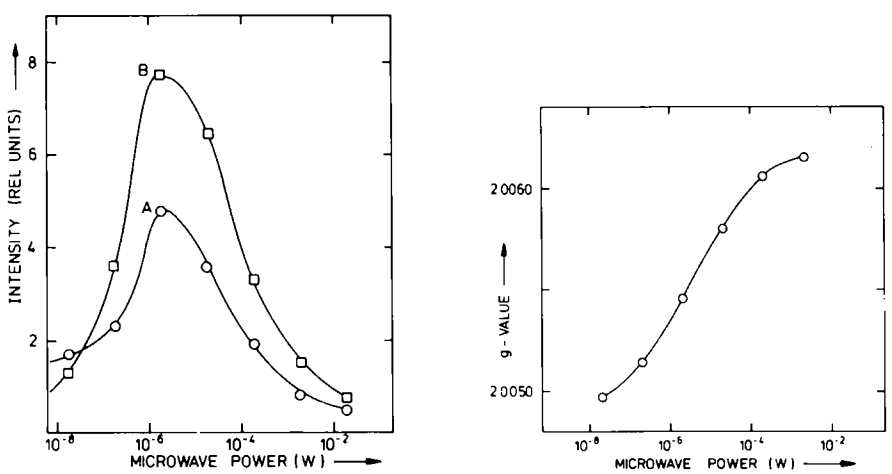

Fig. 3. A. Microwave power saturation at 5 K of the dark ESR signal in AUT-s particles, prepared as in Fig. 2A. B. Microwave power saturation of the light-induced emissive signal of AUT-s particles, prepared as in Fig. 2A.

Fig. 4. Microwave power dependence of the *g*-value of the light-induced emissive ESR signal in AUT-s particles prepared as in Fig. 2A.

power (2 μW, Fig. 3). Surprisingly, upon illumination with continuous white light the sample exhibited an emissive signal (Fig. 2). The emissive line is at low microwave power almost Gaussian. The *g*-value of the emissive signal is dependent on the microwave power (Fig. 4). At 70 dB attenuation it is 2.0049 with linewidth, 7.6 ± 0.4 G. The saturation characteristic of the emissive signal is shown in Fig. 3. Note the signal decrease for high microwave powers ($>2 \cdot 10^{-5}$ W); this effect is due to the fact that the light source is no longer saturating for these microwave powers (see Discussion).

When the sample was warmed up, kept for about one minute at room temperature and subsequently frozen in the dark to 5 K, the normally absorptive signal of P^+ and U_I^- was present under illumination. Warming up again and freezing under illumination made the emissive signal reappear. In Fig. 5 is plotted the intensity at 5 K of the dark and light-induced ESR signal around $g = 2$ vs. the time between illumination and freezing of a sample containing AUT-s particles plus ascorbate. The dependence of the intensity of the emissive signal on the time elapsed before freezing is paralleled by that of the triplet signal arising from the triplet state of the primary donor. Apparently, the appearance of the emissive signal is closely linked to the primary acceptor being reduced, i.e. to the occurrence of the back reaction $P^+I^- \rightarrow P^TI$. The emissive signal was also present in AUT-s particles of *Rps. sphaeroides* reduced in the dark with dithionite, or with 2,3,5,6-tetramethyl-*p*-phenylene diamine while freezing under illumination, in reaction centers of *Rps. sphaeroides* R-26 subjected to treatment with SDS or to the iron-depleting treatment of Okamura [27] and reduced with ascorbate and frozen under illumination, and in chromatophores of *Rps. viridis*, *Rhodospirillum rubrum* and *Chromatium vinosum* incubated with SDS, reduced with ascorbate and frozen under illumination. In the chromatophores the emissive signal was weaker than in the other preparations, probably because the SDS-treatment causes some destruction of the activity of the reaction centers. No emissive signal was found in reaction centers of R-26 or in chromatophores of *Rps. sphaeroides* wild type and R-26 reduced either by dithionite or by ascorbate and light but not incubated with SDS. When no ascorbate or dithionite was added these preparations exhibited the normal signal of P^+ at $g = 2.0026$ together with the well-known signal around $g = 1.83$ and 1.68 due to the reduced primary acceptor complex, $U^-Fe^{2+}(S = 2)$.

From these experiments we conclude that a prerequisite for the induction of the emissive ESR line is the uncoupling of the magnetic interaction between the ubiquinone and the high-spin ferrous ion of the primary acceptor.

If the emissive signal arises because of a polarized light-induced radical that is not present in the dark, then one would expect to observe the absorptive spectrum of the radical once the polarization has decayed by spin-lattice and microwave stimulated relaxation. Thus, in a flash experiment the kinetic trace should first be positive (emissive), then cross the baseline and become negative (absorptive). Fig. 6 shows a kinetic trace of the emissive signal. It rises with the instrumental risetime (20 μs), and decays to zero with halftime of about 20 ms. If for longer times a light-induced absorptive signal is present, then it must be less than one percent of the intensity of the dark ESR line of U_I^- (data not shown). Even at the highest light intensities, no detectable light-induced absorptive signal developed.

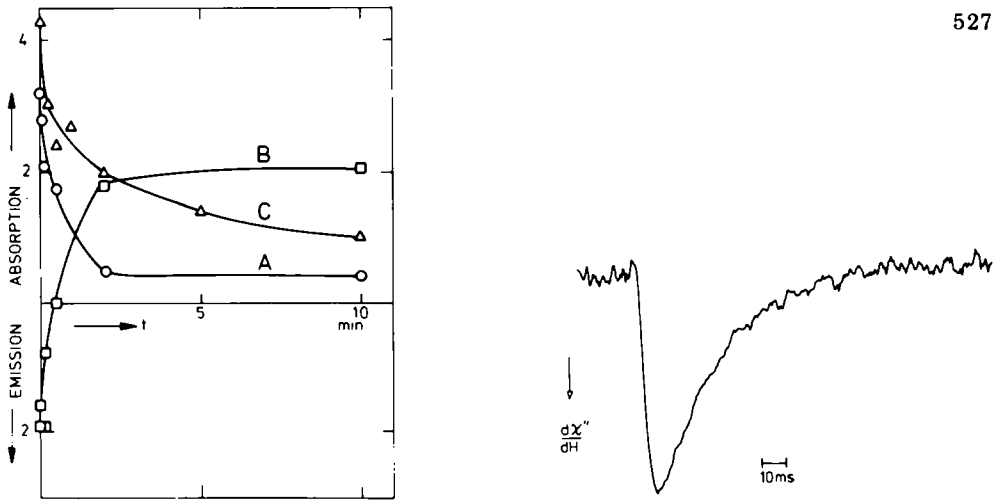

Fig. 5. A. Dark ESR signal of AUT-s particles when ascorbate was added vs. the time between illumination and freezing to 77 K, as measured at 5 K. B. Light-induced emissive ESR signal in AUT-s particles measured at 5 K; conditions and sample preparation as in (A). C. The amplitude of the high field ESR transition H||Z of the triplet state in AUT-s particles measured at 5 K; conditions and sample preparation as in (A).

Fig. 6. Kinetic trace of the light-induced emissive signal in AUT-s particles, prepared as in Fig. 2A, measured after a saturating laser flash. Incident microwave power 10^{-3} mW. Time constant 3 ms.

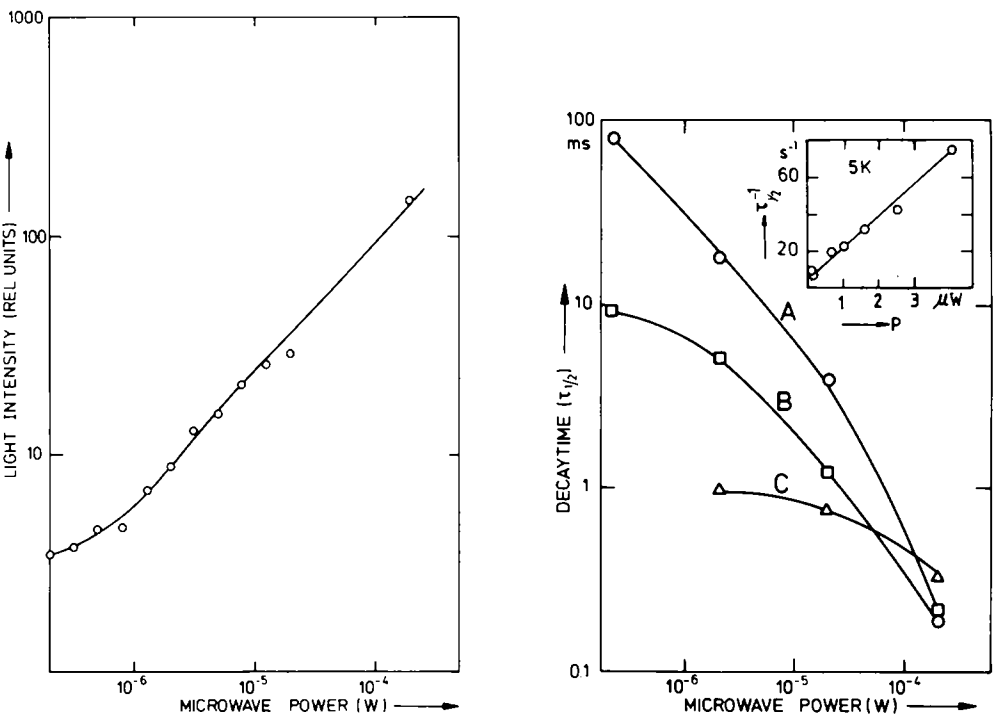

Fig. 7. Plot of the light intensity (white light), for which the light-induced emissive signal has half its amplitude for saturating light vs. the microwave power, measured at 5 K with AUT-s particles to which ascorbate was added before freezing in the light.

Fig. 8. Microwave power dependence of the decay time ($\tau_{1/2}$) of the light-induced emissive signal after a laser flash at different temperatures (A: 5 K; B: 14 K; C: 77 K). The kinetics were measured at the low field peak of the first derivative of the ESR signal. Conditions as in Fig. 2A. Insert: The inverse of the decay time at 5 K plotted vs. the microwave power (linear scale); from this plot T_1 is calculated to be T_1 = 200 ms.

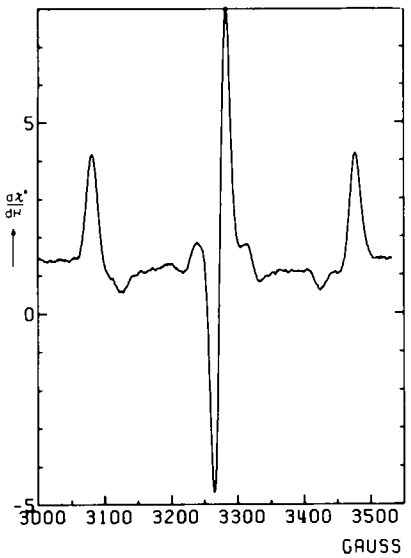

Fig. 9. Light-minus-dark signal of AUT-s particles prepared as in Fig. 2A. Conditions: temperature 5 K, microwave power $2 \cdot 10^{-3}$ W, modulation amplitude 20 G. On the left and right hand of the spectrum one finds the triplet signal of P^T and in the center one finds the emissive signal broadened by the high modulation amplitude.

Fig. 7 shows the light intensity at which the emissive signal in AUT-s particles attains half the amplitude at full light saturation vs. the microwave power. It is seen that at high microwave powers, far more light is needed to half-saturate the emissive signal than at low microwave powers.

The decay time of the emissive signal after a light flash is strongly dependent on the microwave power (Fig. 8) as is expected for a polarized signal. In all preparations that showed the emissive signal, the ESR spectrum of the triplet state of the primary donor, P^T, was also present. Its amplitude and polarization pattern were similar to that observed for P^T in non-treated materials, e.g. bacteria or chromatophores under reducing conditions. However, the lineshape of the spectrum in material that also showed the emissive signal deviated from that of the 'normal' P^T spectrum (Fig. 9). The difference can be attributed to a difference in triplet sublevel decay rates. By flash ESR spectroscopy of AUT-s particles we found for the peak at the canonical Z-direction a value of k_Z roughly half the value of the k_Z found for P^T in chromatophores [31], whereas the values of k_X and k_Y were not significantly altered. The lower value of k_Z for AUT-s particles leads to a higher concentration of the triplet state in molecules with the molecular Z-axis oriented along the magnetic field, and thus to a higher intensity of the Z-ESR line relative to the X- and Y-line as observed. Triplet spectra rather similar to our AUT-s triplet spectra have been reported for other preparations [40].

Discussion

Origin of the emissive ESR signal

Our results show that the appearance of an emissive ESR signal at $g = 2$ is a

general phenomenon in bacterial photosynthetic material in which the magnetic coupling between the primary acceptor and the high-spin ferrous ion is destroyed and in which this primary acceptor has been chemically reduced. We conclude from the *g*-value, the linewidth and the fact that in the reaction center in the state $P^+I^-U^-$ the light-induced radicals P^+ and I^- have lifetimes too short to be detectable on a microsecond or longer timescale [41], that the signal originates from the reduced primary acceptor, U^-, in an emissively polarized state. The signal cannot be due to some other light-induced radical species, because after flash-excitation no absorptive ESR signal is seen with a lifetime exceeding 80 ms. From the curve of the decay time vs. microwave power (Fig. 7), it is seen that at 5 K and at microwave power levels lower than 0.2 μW the emissive signal has a decay time in excess of 80 ms, so that the chemical lifetime of a hypothetical radical other than P^+, I^- or U^- should be longer than 80 ms. Measured after flash excitation at high microwave power, when the decay time of polarization is reduced by stimulated emission to a few ms, the hypothetical radical should show up as an absorptive ESR line, contrary to observation.

The apparent shift of the *g*-value of the emissive signal from 2.005 to 2.006 upon increasing the microwave power is unusual. It is probably caused by a transverse relaxation time T_2 which, at constant power, slightly varies as a function of the resonance frequency, ω. It will be recalled that at low temperatures the lineshape of the ESR lines of ubiquinone is asymmetric [27]; evaluating T_2 as a function of ω by the aid of Eqn. 1 we have observed a shift to faster T_2 in the low field wing of the emissive line. This means that the effective relaxation in the high-field wing is more dominated by stimulated emission at lower microwave power levels than the effective relaxation in the low-field wing, so that the apparent *g*-value is shifted to a slightly higher value at higher microwave power. This effect is analogous to the so-called anomalous saturation reported by Hyde et al. [42].

Triplet

As shown in Fig. 9 the lineshape of the ESR triplet spectrum of P^T differs from the usual spectrum of P^T. This is explained by our finding of a smaller value of k_Z than for whole cells or chromatophores. This 'abnormal' lineshape and the observed emission around $g = 2.00$ are not related to each other, for in a reaction center preparation of R-26 incubated with SDS, emission around $g = 2.00$ was present while the lineshape of the triplet of P^T was 'normal'. From this we conclude that the change of k_Z is due to structural changes in the reaction center during preparation.

Transfer of electron-spin polarization

What is the mechanism by which U^- becomes emissively spin-polarized? This happens most probably by transfer of electron-spin polarization. Pedersen [9] has pointed out that when a spin-polarized radical has an electronic exchange interaction with a radical in Boltzmann equilibrium, one expects only the net polarization to be transferred. The so-called multiplet polarization, which depends on hyperfine interaction, is destroyed by the exchange process because this process does not depend on the nuclear spins. The pure emissivity of the

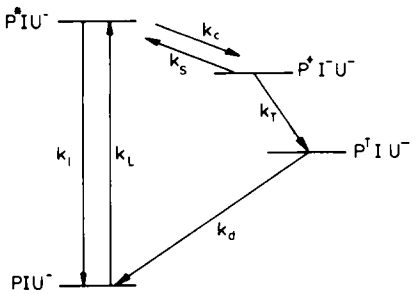

Fig. 10. Schematic representation of primary reactions and their rate constants present in the bacterial photosynthetic system when the primary acceptor has been chemically reduced.

polarized signal reported here, its presence under continuous illumination and the absence of an absorptive line in repetitive flash experiments all are explained by the concept of transfer of polarization by exchange interaction. In the next paragraph, a simple model is worked out in which the intensity of the emissive ESR line is related to the light intensity, the microwave power level, and the exchange rate. In the subsequent sections we will examine to what extent our experimental results support the model.

Transfer of light-induced electron-spin polarization in the bacterial reaction center

The primary reaction in the bacterial reaction center under reducing conditions is schematically depicted in Fig. 10. We assume that in the state $P^+I^-U^-$, I^- is emissively electron-spin polarized and that between I^- and U^- an exchange interaction exists with rate constant k_x. Through this exchange process, the spin polarization of I^- is transferred to U^-, with a probability p given by

$$p = \frac{k_x}{2(k_x + k_T)}$$

The population difference between the upper and lower spin levels of U^- is given by the differential equation:

$$\frac{d\Delta n}{dt} = -\frac{n_B^U + \Delta n}{T_1} - 2\,P\,\Delta n - p \cdot I'[\Delta n + n_B^I(1-\epsilon)] \qquad (2)$$

with $\Delta n = n_+ - n_-$, with n_+ and n_- the population of the upper and lower spin level of U^-, respectively, P the rate of microwave-induced transition, n_B^U and n_B^I the Boltzmann equilibrium population difference of U^- and I^-, respectively, and I' the fraction of intermediary acceptor molecules that is reduced by the light, per second. The factor $(1-\epsilon)$ defines the net polarization of I^-, averaged over the lifetime of the radical pair P^+I^-. For $\epsilon = 0$, I^- is in Boltzman equilibrium, for $\epsilon < 0$ it is absorptively polarized, for $0 < \epsilon < 1$ I^- has a decreased absorption, where for $\epsilon > 1$ I^- is emissively polarized. The first two terms in the right hand side of Eqn. 2 are familiar from the theory of resonant microwave-induced absorption, the third term represents the contribution by electron-spin exchange between I^- and U^-. The steady-state solution of Eqn. 2

is given by:

$$\Delta n = -n_B \cdot \frac{1 + pI'(1-\epsilon)T_1}{1 + 2\,PT_1 + pI'T_1} \tag{3}$$

for $n_B^U = n_B^I = n_B$. This assumption is justified for any two radicals whose resonance frequency and spin-lattice relaxation do not differ appreciably. It is seen that for $P \to 0$ and $\epsilon \to 0$, $\Delta n \to -n_B$, i.e. then exchange does not lead to a change in the distribution of spins over the two spin levels of U^-. I' follows from the steady-state solution of the coupled differential equations which describe the reactions depicted in Fig. 10. This solution is given by

$$I' = \frac{k_c k_L}{ak_L + b} \tag{4}$$

where

$$a = 1 + \frac{k_c}{k_S + k_T}\left(1 + \frac{k_T}{k_d}\right) \tag{5}$$

and

$$b = k_1 + \frac{k_c \cdot k_T}{k_S + k_T} \tag{6}$$

The rate constants k_L, k_1, k_S, k_c, k_T and k_d are defined in Fig. 10.

The expression for the parameters a and b can be simplified considerably when the values of the various rate constants are taken into account. At low temperatures the back reaction to the excited state is inhibited [41]. As the yield of P^T is almost unity below 50 K [41], the decay from P^+I^- to the ground state P I is negligible in our experiments. Thus $k_S << k_T$, whereas k_1, $k_T << k_c$ [16,17]. It follows that $a \sim k_c/k_d$ and $b \sim k_c$. Our maximal intensity of illumination corresponds to $k_L \sim 500\ s^{-1}$, whereas $k_d \sim 10^4\ s^{-1}$ at low temperatures [29]. Thus $k_L/k_d << 1$ and $I' \sim k_L$. Substituting $I' = k_L$ in Eqn. 3 we obtain

$$\Delta n = -n_B \cdot \frac{1 + p(1-\epsilon)k_L \cdot T_1}{1 + 2\,PT_1 + pT_1k_L} \tag{7}$$

For most experiments we have monitored the difference between the dark (absorptive) ESR signal and the light-induced (emissive) signal. Denoting the difference between Δn in the light and Δn in the dark by Δn_e, we have

$$\Delta n_e = \Delta n + \frac{n_B}{1 + 2\,PT_1} \tag{8}$$

or

$$\Delta n_e = \frac{n_B p k_L T_1 [1 - (1-\epsilon)(1 + 2\,PT_1)]}{(1 + 2\,PT_1 + pk_L T_1)(1 + 2\,PT_1)} \tag{9}$$

From Eqn. 9 it is readily seen that for values of k_L such that pk_LT_1 exceeds $1 + 2\,PT_1$, the exchange induced excess population difference of U^- saturates to a maximum value of

$$\frac{n_B}{1 + 2\,PT_1} + n_B(\epsilon - 1)\,.$$

For moderate values of P the light-induced ESR amplitude is proportional to $P^{1/2}$ so that

$$A \propto P^{1/2} \cdot \Delta n_e$$

or

$$A^{-1} \propto c_1 + c_2 k_L^{-1} \tag{10}$$

with

$$c_1 = P^{-1/2} \cdot \frac{(1 + 2\,PT_1)}{n_B[1 + (\epsilon - 1)(1 + 2\,PT_1)]}$$

$$c_2 = P^{-1/2} \cdot \frac{(1 + 2\,PT_1)^2}{n_B p T_1[1 + (\epsilon - 1)(1 + 2\,PT_1)]}$$

Thus, a plot of A^{-1} vs. k_L^{-1} yields a straight line. From the slope, information on p, i.e. on k_x, and on the polarization factor $(\epsilon - 1)$ can be obtained. More conveniently, p can be determined by measuring as a function of microwave power the light intensity, k_L^*, at which the emissive signal has half its maximal intensity. From Eqn. 9 it follows that

$$k_L^* = \frac{1}{pT_1}(1 + 2\,PT_1) \tag{11}$$

Thus, a plot of k_L^* vs. P in s^{-1}, yields a straight line with slope $2/p$, which intersects the k_L^* axis at $k_L^* = 1/pT_1$ $(P = 0)$. In practice, a plot of $\log(k_L^* - (1/pT_1))$ vs. $\log P$ is used, which yields a straight line with slope unity.

The dependence of emissivity on light intensity and on microwave power

Eqn. 10 gives the amplitude A of the light-minus-dark ESR signal as a function of the average number of light quanta absorbed per second, k_L. A plot of A^{-1} vs. k_L^{-1} should yield a straight line, the slope of which varies with microwave power. From Fig. 11 it is seen that this relation is obeyed with good accuracy by the experimental results.

The relation between the light intensity at which one-half of the maximum amplitude of the emissive signal is obtained, and the microwave power is given by Eqn. 11. A plot of $\log(k_L^* - (1/pT_1))$ vs. $\log P$ should result in a straight line with slope unity. Fig. 12 shows that our data fit Eqn. 11 reasonably well, the measured slope being 0.8. The agreement is gratifying, considering the low amplitude of the emissive line at high P and the difficulty in light-saturating the signal under these conditions.

We conclude that our experimental data are well described by the model.

Estimate of the exchange rate, k_x

A direct but hazardous way of determining k_x is the plot corresponding to Eqn. 11 (Fig. 12). The intercept of the straight line in the log-log plot gives the ratio $4\,k_x/(k_x + k_T)$ directly, provided P is calibrated in s^{-1}. This requirement is severe, in view of the notorious difficulty to accurately determine the intensity of the microwave field at the location of the sample inside the cavity. Less directly, k_x can be determined from the plot of k_L^* vs. P in the limit of $P \to 0$.

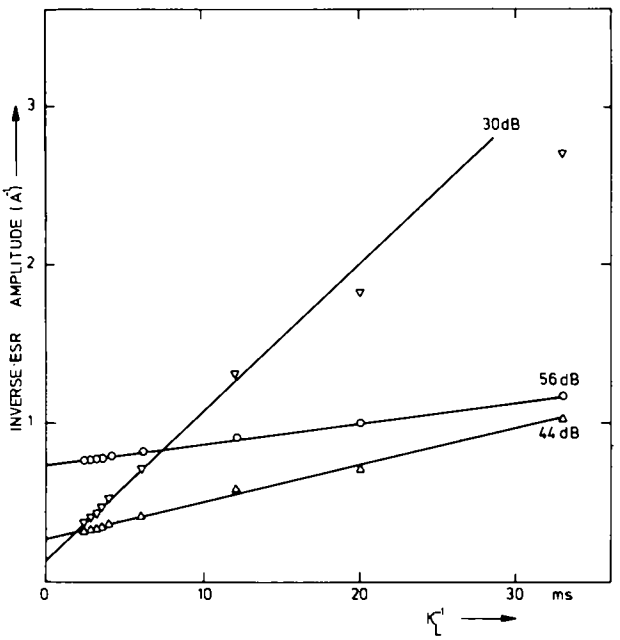

Fig. 11. Light saturation plot of the emissive ESR signal at different microwave powers, with the inverse ESR signal plotted vs. the inverse of the light intensity. Sample prepared as in Fig. 2A.

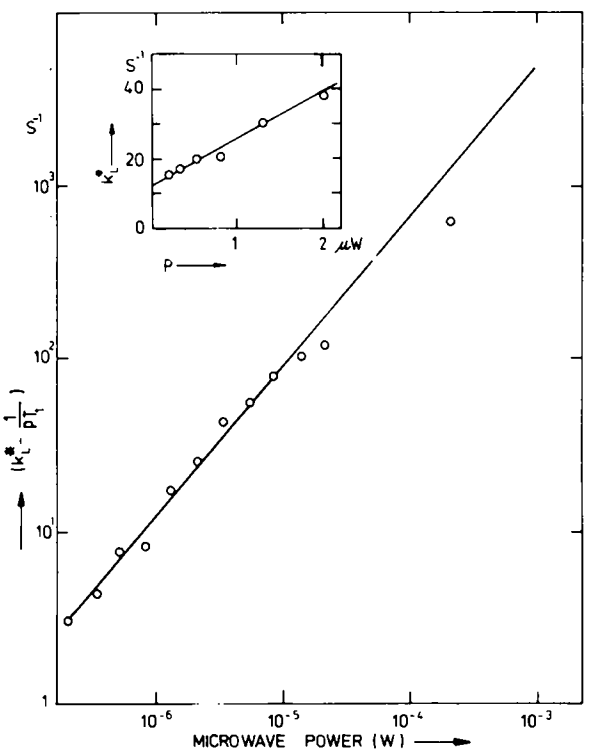

Fig. 12. A plot of $k_L^* - (1/pT_1)$ (see text) vs. the microwave power. Insert: A linear plot of k_L^* vs. the microwave power; from this plot k_x is calculated.

The intersection of the straight line in Fig. 12 (insert) with the k_L^* axis yields $T_1 \cdot k_x/2(k_x + k_T) = 0.08$. T_1 was estimated to be 200 ms from the decay of the emissive signal after a laser flash, extrapolated to $P \to 0$. It follows that $k_x/(k_x + k_T) = 0.8$, which yields, with $k_T = 10^8\ s^{-1}$, $k_x \sim 4 \cdot 10^8\ s^{-1}$. This value may be compared with the electron transport data of Okamura et al. [17] for the reaction $I^- U^- \to I\ U^{=}$. These authors derive for the exchange matrix element $|T_{ab}|$ a value of $1.3 \cdot 10^{-4}$ eV. $|T_{ab}|$ is related to the Heisenberg exchange integral J by [17]:

$$J = -\frac{2|T_{ab}|^2}{(E_a - E_b - \Delta)} \tag{12}$$

where $E_a - E_b$ is the difference in redox midpoint potential of species a and b and Δ is the Franck-Condon parameter.

Applying Fermi's golden rule we can write

$$k_x = \frac{2\pi}{\hbar} J^2 \rho(E)\ ,$$

where $\rho(E)$ is the density of states. For the present case $\rho(E)$ is given by the inverse of the ESR linewidth, which can be approximated by J for an exchange interaction of the order of or exceeding the hyperfine interaction. Thus,

$$k_x \sim \frac{4\pi}{\hbar} |T_{ab}|^2/|E_a - E_b - \Delta| \sim \frac{2\pi}{\hbar} |T_{ab}|^2 \text{ for } |E_a - E_b - \Delta| \sim 2 \text{ eV [17]}\ ,$$

yielding $k_x \sim 1.6 \cdot 10^8\ s^{-1}$. The agreement with our value of k_x is satisfactory and lends additional support to the validity of our model.

From our value of k_x it follows that $T_{ab} = 2 \cdot 10^{-4}$ eV. Using the approximate relations between T_{ab} and distance given by Hopfield [43] and Jortner [44], this corresponds to a distance between I^- and U^- of 10—11 Å, in agreement with previous estimates [17,45]. Finally we note that from Eqn. 12 it follows that the exchange interaction between I^- and U^- is about 3—5 G, again in good agreement with the value 1.8 G by Okamura et al. [17].

Acknowledgements

We are indebted to Dr. L.N.M. Duysens for his continuous interest. One of us (A.J.H.) acknowledges helpful discussions with Dr. J.B. Pedersen. R.H. Voogd and A.H.M. de Wit expertly prepared the reaction center preparations. We are grateful to those authors who sent us preprints of their recent work.

This research was supported by the Netherlands Foundation for Chemical Research (SON) with financial aid from the Netherlands Organization for the Advancement of Pure Research (ZWO).

References

1 Blankenship, R.E., McGuire, A. and Sauer, K. (1975) Proc. Natl. Acad. Sci. U.S.A. 72, 4943—4947
2 McIntosh, A.R. and Bolton, J.R. (1976) Nature 263, 443—445
3 Hoff, A.J., Gast, P. and Romijn, J.C. (1977) FEBS Lett. 73, 185—190
4 Dismukes, G.C., McGuire, A., Blankenship, R. and Sauer, K. (1978) Biophys. J. 21, 239—256

5 Adrian, F.J. (1977) in Chemically Induced Magnetic Polarization (Muus, L.T., Atkins, P.W., McLaughlan, K.A. and Pedersen, J.B., eds.), Chapter 5, D. Reidel, Dordrecht
6 Blankenship, R.E., Schaafsma, T.J. and Parson, W.W. (1977) Biochim. Biophys. Acta 461, 297—305
7 Hoff, A.J., Rademaker, H., van Grondelle, R. and Duysens, L.N.M. (1977) Biochim. Biophys. Acta 460, 547—554
8 Haberkorn, R., Michel-Beyerle, M.E. (1977) FEBS Lett. 75, 5—8
9 Pedersen, J.B. (1979) FEBS Lett. 97, 305—310
10 Friesner, R., Dismukes, G.C. and Sauer, K. (1979) Biophys. J. 25, 277—294
11 McIntosh, A.R., Manikowski, H., Wong, S.K., Taylor, C.P.S. and Bolton, J.R. (1979) Biochem. Biophys. Res. Commun. 87, 605—612
12 McIntosh, A.R. and Bolton, J.R. (1979) Rev. Chem. Intermediates, in the press
13 Dutton, P.L., Leigh, J.S. and Seibert, M. (1971) Biochem. Biophys. Res. Commun. 46, 406—413
14 Thurnauer, M.C., Katz, J.J. and Norris, J.R. (1975) Proc. Natl. Acad. Sci. U.S.A. 72, 3270—3274
15 Kaufmann, K.J., Dutton, P.L., Netzel, T.L., Leigh, J.S. and Rentzepis, P.M. (1975) Science 188, 1301—1304
16 Rockley, M.G., Windsor, M.W., Cogdell, R.J. and Parson, W.W. (1975) Proc. Natl. Acad. Sci. U.S.A. 72, 2251—2255
17 Okamura, M.Y., Isaacson, R.A. and Feher, G. (1979) Biochim. Biophys. Acta 546, 394—417
18 Hoff, A.J. and Gast, P. (1977) 4th Int. Congr. on Photosynthesis, Reading, England, Abstr. 163
19 Cohen-Bazire, G., Sistrom, W.R. and Stanier, R.Y. (1957) J. Cell. Comp. Physiol. 49, 25—68
20 Hendley, D.D. (1955) J. Bacteriol. 70, 625—634
21 De Klerk, H., Bartsch, R. and Kamen, M.D. (1965) Biochim. Biophys. Acta 97, 275—280
22 Romijn, J.C. and Amesz, J. (1977) Biochim. Biophys. Acta 461, 327—338
23 Loach, P.A., Sekura, D.L., Hadsell, R.M. and Stemer, A. (1970) Biochemistry 9, 724—733
24 Slooten, L. (1972) Biochim. Biophys. Acta 256, 452—466
25 Slooten, L. (1973) Thesis, University of Leiden
26 Okamura, M.Y., Steiner, L.A. and Feher, G. (1974) Biochemistry 13, 1394—1402
27 Feher, G., Okamura, M.Y. and McElroy, J.D. (1972) Biochim. Biophys. Acta 267, 222—226
28 Visser, J.W.M. (1975) Thesis, University of Leiden
29 Parson, W.W. and Monger, T.G. (1976) Brookhaven Symp. Biology 28, 195—212
30 Wraight, C.A., Leigh, J.S., Dutton, P.L. and Clayton, R.K. (1974) Biochim. Biophys. Acta 333, 401—408
31 Gast, P. and Hoff, A.J. (1978) FEBS Lett. 85, 183—188
32 Romijn, J.C. and Amesz, J. (1976) Biochim. Biophys. Acta 423, 164—173
33 Atkins, P.W., McLauchlan, K.A. and Percival, P.W. (1973) Mol. Phys. 25, 281—296
34 Weger, M. (1960) Bell. Syst. Techn. J. 39, 1013—1112
35 Feher, G. (1956) Phys. Rev. 114, 1219—1244
36 Loach, P.A. and Hall, R.L. (1972) Proc. Natl. Acad. Sci. U.S.A. 69, 786—790
37 Vermeglio, A. (1977) Biochim. Biophys. Acta 459, 516—524
38 Wraight, C.A. (1977) Biochim. Biophys. Acta 459, 525—531
39 Blankenship, R.E. and Parson, W.W. (1979) Biochim. Biophys. Acta 545, 429—444
40 Prince, R.G., Dutton, P.L., Clayton, B.J. and Clayton, R.K. (1978) Biochim. Biophys. Acta 502, 354—358
41 Parson, W.W., Clayton, R.K. and Cogdell, R.J. (1975) Biochim. Biophys. Acta 387, 265—278
42 Hyde, J.C., Erikson, L.E.F. and Ehrenberg, A. (1970) Biochim. Biophys. Acta 222, 688—691
43 Hopfield, J. (1974) Proc. Natl. Acad. Sci. U.S.A. 71, 3640—3644
44 Jortner, J. (1976) J. Chem. Phys. 64, 4860—4867
45 Peters, K., Avouris, P. and Rentzepis, P.M. (1978) Biophys. J. 23, 207—217